Entropy of Acoustical Beams in a Random Ocean

Andrey Morozov and John Colosi

Woods Hole Oceanographic Institution, Woods Hole MA 02543
e-mail: amorozov@whoi.edu, jcolosi@whoi.edu

***Abstract*-Scattering by small scale ocean processes like internal waves imposes the ultimate limitations on large scale ocean acoustic remote sensing. Recent progress in utilizing ray methods to understand scattering processes in long range acoustic propagation suggest there is an exponential sensitivity to initial conditions and a rapid growth of acoustic field complexity with a scale of a few hundred kilometers; a result which casts some doubt on the effectiveness of long range acoustic remote sensing. However, as is well known in other fields of wave propagation, finite frequency effects can slow, suppress or mask this complexity. We have performed parabolic equation numerical simulations for acoustical beams which mimic a narrow bundle of ray paths and which traverse random realizations of internal wave sound speed perturbations obeying the Garrett-Munk internal wave spectrum. The variability of these beams as a function of range and beam angle are analyzed in terms of information theory using the Shannon entropy and in terms of the relative intensity variance or scintillation index. We find that the finite frequency beams do not increase in complexity exponentially and that very near the saturation range a constant non-maximal entropy is obtained. These results suggest that acoustic remote sensing is more robust than is implied by the ray scattering results.**

I. INTRODUCTION

It is well known that acoustic energy in the ocean is significantly scattered by sound speed fluctuations induced by internal waves. The statistics of sound fluctuations in a random ocean defines a structure of optimal signal processing algorithms and the potential characteristics of remote sensing systems. The stochastic properties of the sound field scattered by internal waves are poorly understood in long-range propagation as conditions of saturation are established. Ray theory suggests that acoustic trajectories can be very sensitive to small perturbations of the initial conditions and media parameters (similar to light speckle sensitivity to a mirror rotations). For long distances this effect leads to exponential increase of the acoustic field complexity and to chaos of ray's trajectories.

The objective of this paper is to examine the phenomenon of ray chaos and its potential manifestations in finite frequency wave fields.

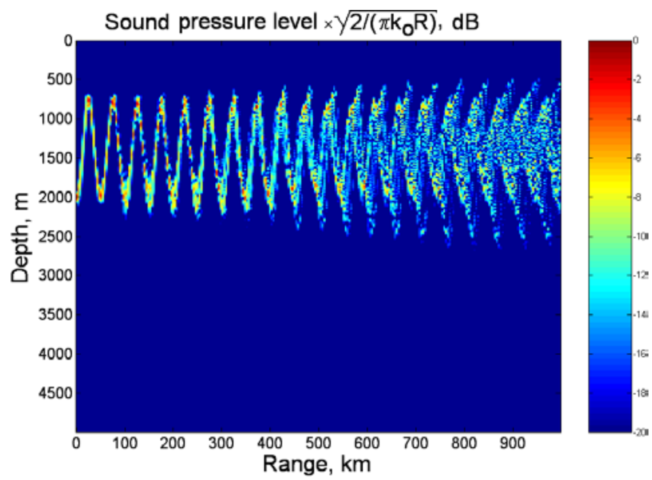

Fig. 1 Explosive acoustical beam.

This problem was initially considered by Tappert [1], where he showed that the width of a narrow-angle beam propagating through a strong mesoscale sound-speed field tends to increase exponentially (explosively) with range at a rate that is predicted by the geometric Lyapunov exponent.

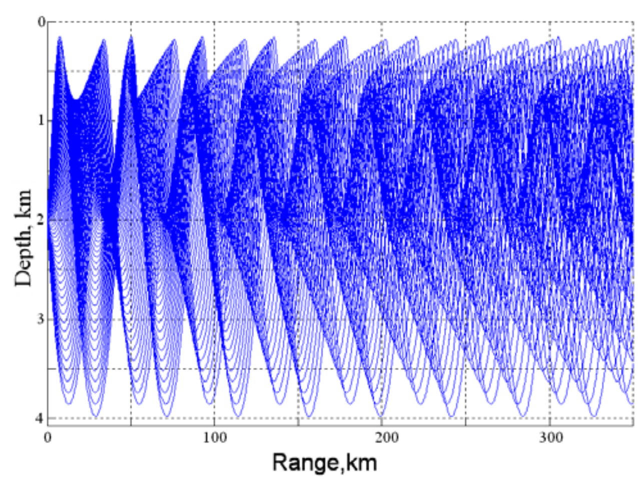

Fig. 2 Concentration of ray trajectories along the weakly divergent bundle of rays.

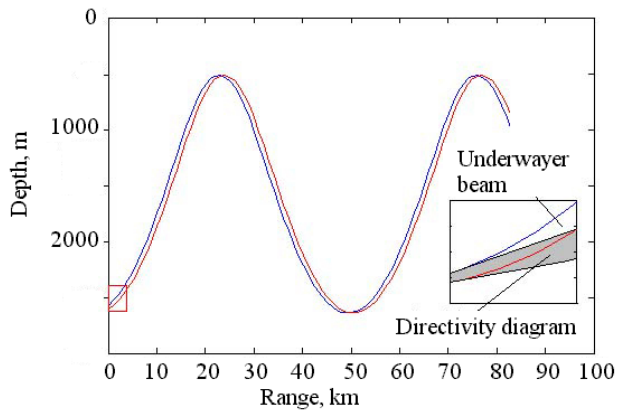

Fig.3 Physical explanation of weakly divergent beam generation.

An example of such an explosive beam in an internal wave environment is shown in Fig. 1. In this paper we investigate the implications of ray chaos for the case of narrow acoustic beam scattering by a realistic random internal-wave field.

The organization of the paper is as follows. In section II the narrow angle beam is described. In section III the acoustic propagation and internal wave models which are the basis of the Monte Carlo method are discussed. In section IV the range evolution of intensity statistics are described, while section V presents results on wavefront complexity. Section VI has summary and conclusions.

II. WEAKLY DIVERGENT BEAMS

The existence of weakly divergent bundles of rays was discovered and described in [2-4].

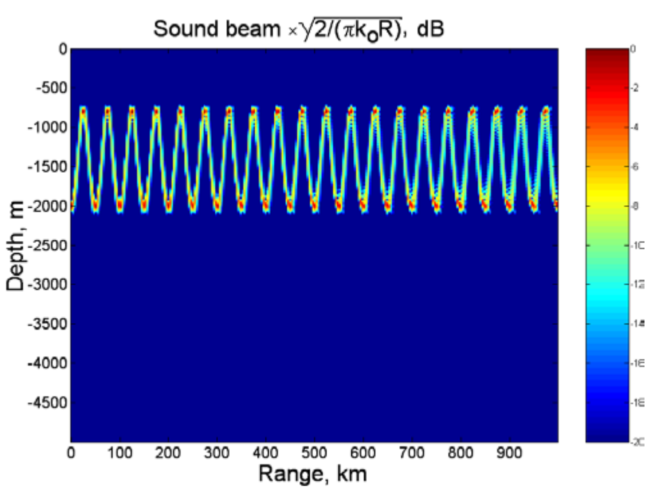

Fig. 4 Weakly divergent narrow acoustical beam.

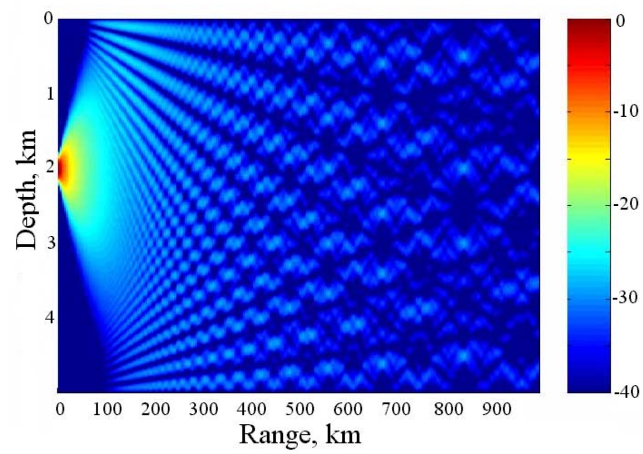

Fig. 5 Sound emitted by the same aperture in a homogeneous medium with the constant background sound speed.

Long-range propagation experiments often showed strong increases of sound intensity at different depths far from the axis of the underwater channel. This phenomenon was explained by focusing of acoustical energy along weakly divergent bundles of rays. Rays comprising this bundle are grouped around a central ray with the turning point at the source depth, i.e. the beam emerges horizontally from the source. When a sound source is near the channel, this bundle corresponds to the usual energy concentration along the channel.

The angle α_s of a weakly divergent bundle of rays are close to points of smooth extremum of the angular dependence of a ray cycle length $D(\alpha_s)$ [2].

In Fig.2 one can see how energy and ray trajectories are concentrating near the direction of weakly divergent bundle of rays. Such concentration can be found in any horizontally homogeneous ocean profile and this property remains (in the adiabatic approach) for small horizontal gradients of sound speed. The geometrical acoustics interpretation of a narrow weakly divergent bundle of rays is demonstrated in Fig.3. Suppose that the source radiation width is confined by crossing trajectories of two acoustic rays shifted in the horizontal direction by a small distance roughly equal to the horizontal width of bundle, then the sound energy will spread in the narrow path bounded by those rays. The sound source with such directivity will form a narrow weakly divergent beam radiated at zero initial angle. This property can be used to simulate a very narrow angle beam emitting from a finite aperture. It can be achieved by variation of the initial Gaussian beam width until the condition of a weakly divergent beam is satisfied. Each turning point acts like a local focusing lens. The focusing effect partially compensates the diffractive expansion thereby forming the weakly divergent beam. An example of a 250 Hz weakly divergent beam is shown in figure 4. The vertical dimension of the sound source aperture is roughly

150 m. The sound from a source with the same aperture as figure 4 was numerically simulated in a homogeneous medium $c(z) = c_0, -H < z < 0$, where H is the ocean depth (Fig.5). A comparison between figs 4 and 5 shows that in a waveguide even a relatively small aperture sound source can concentrate energy (single frequency!) in a very narrow beam. The same property can be used in receiving arrays for forming super resolution directivity by taking into account sound speed profile $c(z)$ measured near the receiver.

The concentrated narrow angle beam is a simple and interesting subject for numerical simulation of acoustic energy scattering by internal waves.

III. ACOUSTIC PROPAGATION ENVIRONMENT

The sound speed as a function of range (x), and depth (z) is defined by the sum:

$$c(x,z) = c_m(z) + \partial c(x,z)\,, \qquad (1)$$

where $c_m(z)$ is the mean sound speed profile and $\partial c(x,z)$ is a random perturbation induced by internal waves. For simplicity a Munk canonical model is used for the mean profile and, the internal wave contribution is modeled using the Garrett-Munk spectrum which has been described in detail by Colosi and Brown [5]. For the buoyancy frequency, $N(z)$, a canonical form is also used such that, $N(z) = 6\exp(z/1300)$ cph. The internal wave energy was normalized so that at the depth, where $N(z^*) = 3\ cph$, the mean square perturbation is equal to $<\xi^2(z^*)> = (7.3)^2\ \mathrm{m}^2$.

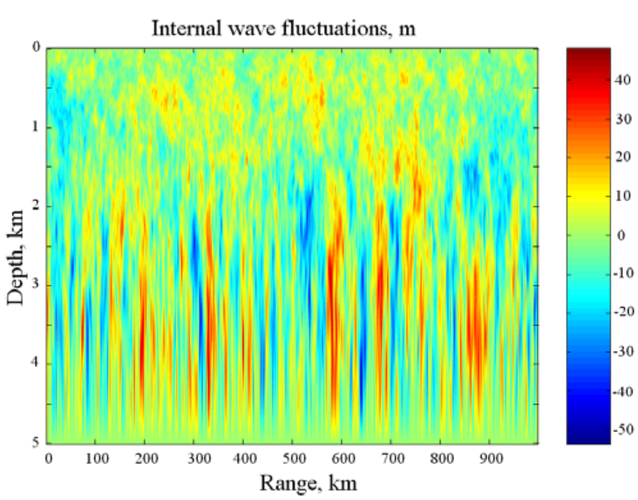

Fig. 6 The field of internal wave displacements.

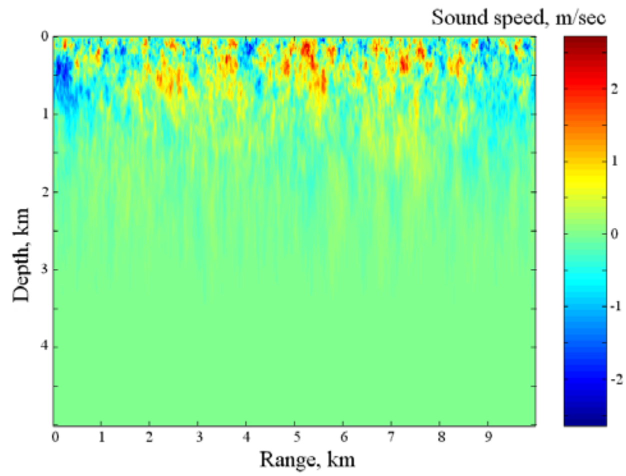

Fig. 7 A realization of internal wave sound speed fluctuations.

In further analysis we will also use sound-speed perturbations with four times more energy (variance), such fluctuations will be called strong sound-speed fluctuations. The more energetic case will be denoted in further references as strong sound-speed fluctuations. An example of one realization of the modeled random field of internal wave displacements is shown in Fig 6. The sound speed fluctuations induced by this internal wave fluctuation field are shown in Fig. 7.

Two hundreds realizations of the random sound speed field were calculated and used to compute two hundred realizations of the acoustic pressure field at each location in space out to 1000 km.The acoustic frequency was 250 Hz. The propagation modeling was carried out using a wide-angle Greens function approach [6], and all cylindrical spreading factors were removed.

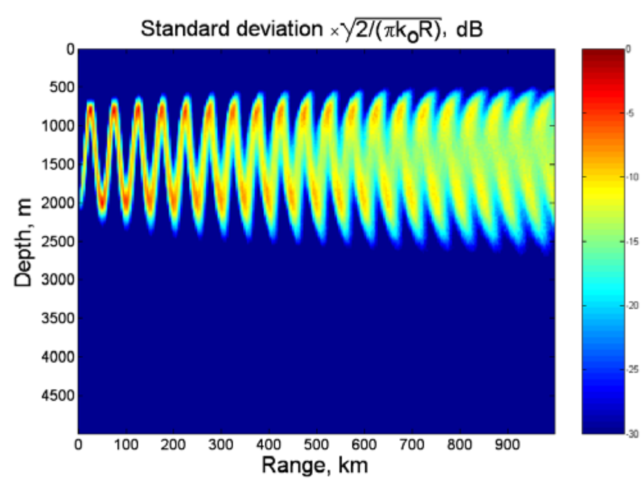

Fig. 8 Standard deviation of sound pressure for a beam.

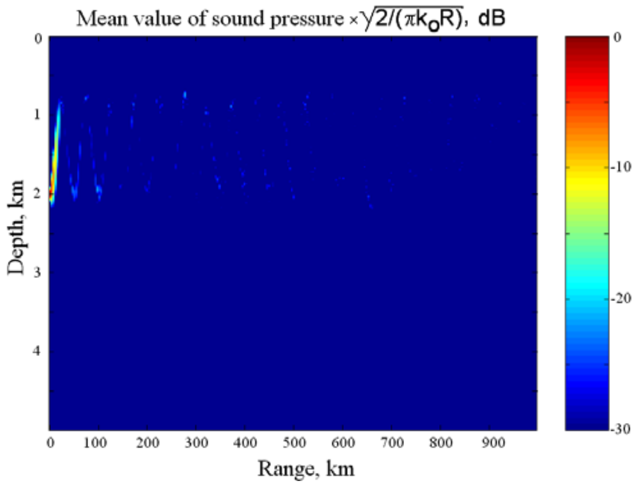

Fig. 9 Acoustic field mean value.

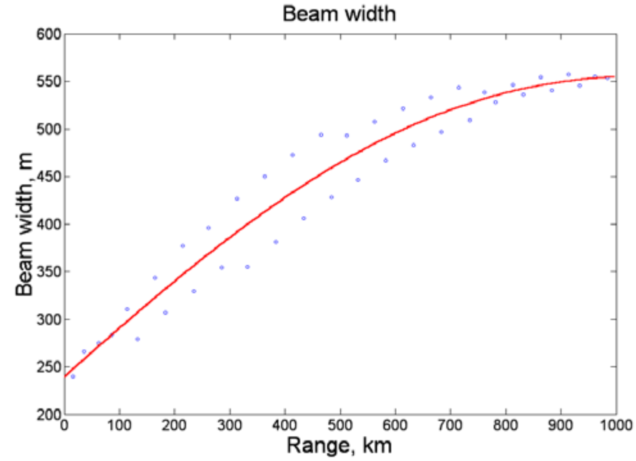

Fig.11 Acoustical beam width.

IV. INTENSITY FLUCTUATIONS

The spatial distribution of rms acoustical fluctuation (dB) of the beam for the normalized internal wave field is shown in Fig. 8; the mean field shown in Fig. 9 is essentially zero after the first 50 km. The acoustical energy is seen to scatter and diffuse from the narrow path. The beam width increases in accordance with [1] and at a distance close to 1000 km the beam expansion appears to have slowed considerably. As a result of scattering the spatial spectrum expands (Fig. 10). The dependence of mean-square beam width and angle spectrum width vs range are shown in Fig. 11 and 12. The beam and its spectrum expand linearly at short ranges and stop increasing near the final range.

The scintillation index (SI),

$$SI(x,z) = (< I^2(x,z) > - < I(x,z) >^2) / < I(x,z) >^2, \quad (2)$$

allows examination of the approach to strong wave scattering or saturation where $z = f(x)$ is the center ray trajectory of a narrow weakly divergent bundles of rays. Here < > is an averaging operator over the 200 realizations and $I(x,z)$ is the sound intensity. The scintillation indexes are shown in Fig. 13; blue is for the standard internal wave energy level and red is for the strong internal waves. Scintillation index is one for Gaussian random noise. SI is approaching one for both cases and demonstrates the saturation process.

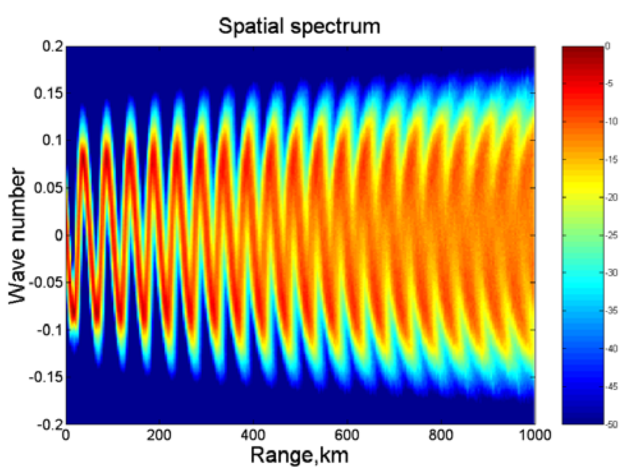

Fig. 10 Wave-number k_z spectrum.

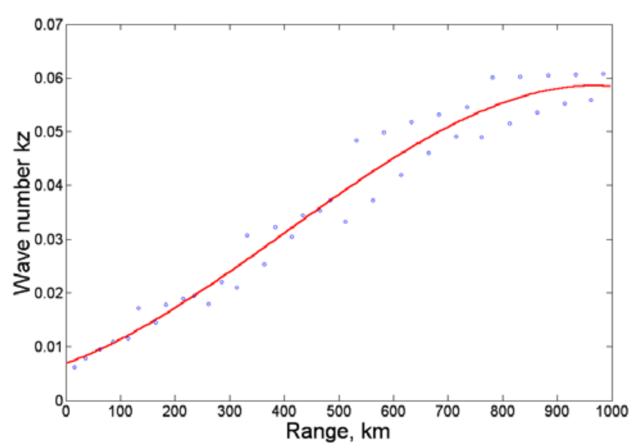

Fig. 12 Wave-number spectrum width.

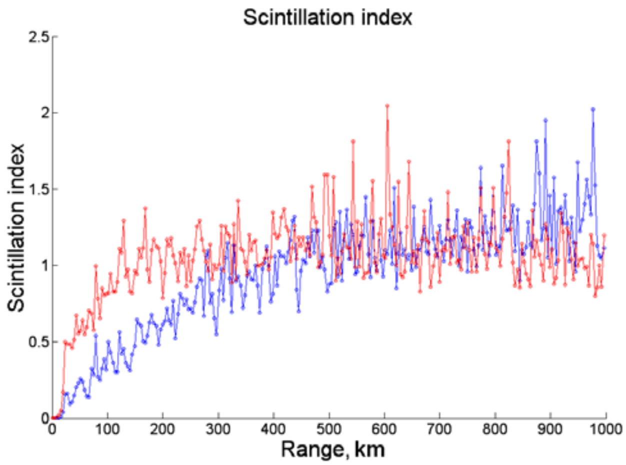

Fig. 13 Scintillation index in the beam center for weak (blue) and strong (red) internal wave fields.

For the standard internal wave energy the scintillation index increases above one at a distance of approximately 300 km and then approaches one from above. The more energetic internal wave field, however does not display the approach from above one.

V. WAVE CHAOS COMPLEXITY

The complexity of a random process depends on the number of independent components of a Karhunen-Loeve (KL) expansion. The sound pressure $s(x,z)$ of an acoustical field in each section $x = const$ can be represented by a stochastic series with $N(x)$ significant contributions,

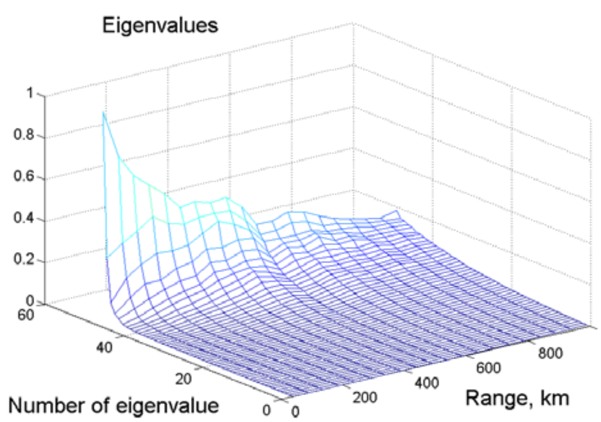

Fig. 14 Dependence of eigenvalues $\lambda_j(x)$ on range.

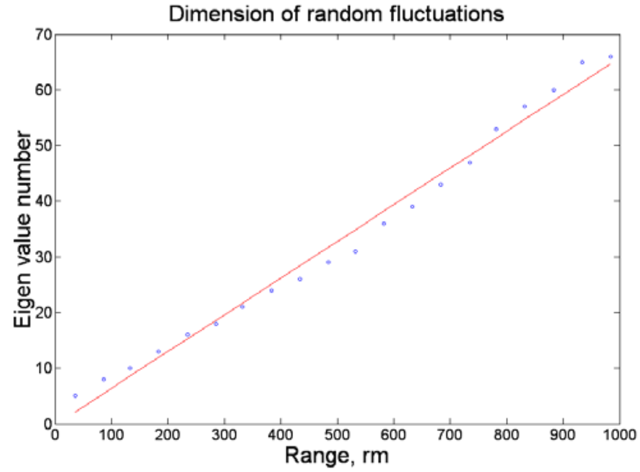

Fig. 15 Dimension of random fluctuations as a function of range.

$$s(x,z) = \sum_{j=1}^{N(x)} \alpha_j(z)\Phi_j(x,z); \qquad (3)$$

where:

$$\alpha_j(x) = \int_{-H}^{0} s(x,z)\Phi_j(x,z)dz; \qquad (4)$$

$$\lambda_j(x)\Phi_j(x,z) = \int_{-H}^{0} K(z,\tilde{z},x)\Phi_j(x,\tilde{z})d\tilde{z};$$

$$K(z,\tilde{z},x) = < p(x,z)p^*(x,\tilde{z}) >; \qquad (5)$$

$K(z,\tilde{z},x)$ is the transverse correlation function for section $x = const$; $\lambda_j(x)$ and $\Phi_j(x,z)$ are the eigenvalues and eigen functions of the KL expansion at range x. The functions $\lambda_j(x)$ and $N(x)$ are shown in Figs. 14 and 15. Note, that curves for the angle spectrum width and number of significant KL expansion components both can be used as an approximate measure of random process. More precisely the logarithym of complexity of a stochastic process is measured by the entropy (E),

$$\mathrm{E(x) = -< P(S(x)Log_2P(S(x)) >}; \qquad (6)$$

where $S(z)$ is the set of sound pressure values in the section $x = const$, and $\mathrm{P(S(x))}$ is the probability of that set. The calculation of sound pressure entropy directly by Monte Carlo stochastic simulation needs a large number of realizations to define P(S) and is computationally intensive. A simplified approach based on the Gaussian approximation of the acoustical fluctuations will be used; that is the entropy will be calculated as if P is Gaussian. The entropy of a single Gaussian variable with standard deviation σ and mean value m can be calculated by formula (6), yielding the analytic result,

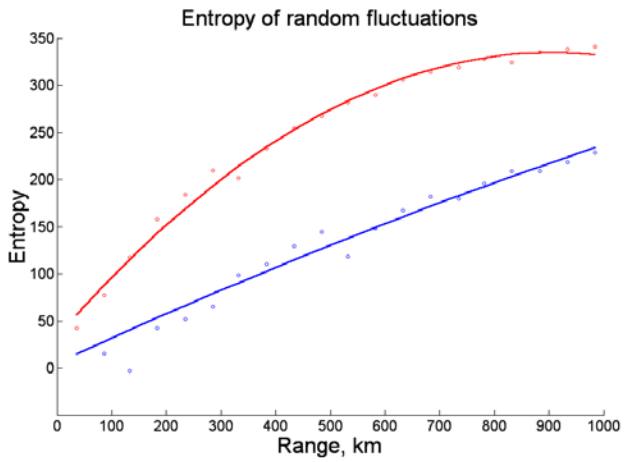

Fig. 16 Entropy of sound pressure fluctuations for weak (Blue) and strong (Red) internal-wave fluctuations.

$$E = -\int_{-\infty}^{+\infty} \frac{e^{-\frac{(s-m)^2}{2\sigma^2}}}{\sqrt{2\pi\sigma^2}}[\frac{1}{2}\log_2 2\pi\sigma^2 + \frac{(s-m)^2}{2\sigma^2}\log_2 e]ds = 0.5\log_2 2\pi e\sigma^2 \quad (7)$$

The entropy of the sound pressure in this Gaussian approximation is equal to the entropy of the random vector $\{\lambda_1(x), \lambda_2(x), ...\lambda_{N(x)}(x)\}$ with the KL eigenvalues. Thus

$$E(x) = E(\lambda_1(x), \lambda_2(x), ...\lambda_{N(x)}(x)) = \sum_{j=1}^{N(x)} \frac{1}{2}\log_2 2\pi\lambda_j(x) \quad (8)$$

where λ_j are the eigenvalues, $j = 1,2,...N(x)$. For equipartition of energy $\lambda_j = \lambda$ (eigenvalue spectrum "white") and the entropy is maximum $E = E_m$, otherwise λ_j is some distribution and $E < E_m$. The eigenvalue spectrum from the simulations is shown in Fig. 14. The spectrum expands with range, but even at the distance 1000 km it remains non-uniform ("not white").

The entropy of the narrow weakly divergent sound beam is shown in Fig. 16 for both the strong and normalized internal wave fields. At short range the entropy increases linearly. This means that the number of equi-probable states of the dynamical system is increasing exponentially in complete accordance with ray chaos theory. The level of scintillation index at the same distances shows that the fluctuations are not saturated in that range. For the strong internal wave case and close to saturation (i.e. longer ranges) the linear behavior disappears and the entropy stabilizes (but not at the maximal value). The scintillation index curves (Fig 13) show that nearly at the same ranges the random process approaches saturation. The stabilization of entropy shows that when fluctuations approach saturation, ray chaos phenomenon is arrested and that the scattering processes in this case are more complicated. In summary, manifestations of ray chaos are evident at short ranges, where the entropy gradient is constant, but at large distances the complexity stabilizes as fluctuations approach saturation.

VI. CONCLUSION

Monte Carlo stochastic simulation of acoustic scattering by internal-waves allows analysis of the variability of weakly divergent beam as a function of range. The analysis was performed in terms of Shannon information theory using the entropy as a measure of complexity and in terms of the relative intensity variance or scintillation index. Finite frequency beams are seen to increasing exponentially in complexity only at short range; this can be considered as a validation of "ray chaos" phenomenon. At saturation the gradient of entropy decreases and constant non-maximal entropy is obtained. These results suggest that near the saturation range the scattering process is more complicated than simple ray chaos and will involve diffractive effects.

References

[1] F. Tappert, Explosive beam spreading due to ray chaos, J. Acoust. Soc. Am., Vol. 106, Issue 4, p. 2225, (1999).
[2] L.. M. Brekhovskih, et al., Long-Range Propagation Experiments in the Canary Hollow of the Atlantic Ocean, Akust. Zh., 1990, vol.36, no 5.
[3] V. V. Goncharov, V. M. Kurtepov Formation and propagation of weakly diverging bundles of rays in a horizontally inhomogeneous ocean. Acoustical Physics 1994, vol. 40, N 5.
[4] Yu. V. Petukhov A sound beam with minimal wave front divergence in a stratified ocean waveguide. Acoustical Physics 1994, vol. 40, N 1.
[5] J. A. Colosi, M. G. Brown Efficient numerical simulation of stochastic internal-wave induced sound-speed perturbation fields. J. Acoust. Soc. Am., Vol. 103, Issue 4, (1998).
[6] F. B. Jensen, W. A. Kuperman, M. B. Porter, H. Schmidt Computation ocean acoustics, AIP series in modern acoustics and signal processing. Springer-Verlag New York, Inc. 2000.
[7] C. E. Shannon, ``A mathematical theory of communication," Bell System Technical Journal, vol. 27, July and October, 1948.